Core−Shell-Shaped Organic−Inorganic Hybrid as Pore Generator for Imprinting Nanopores in Organosilicate Dielectric Films

Chen Hong-Ji*,†,‡ and Fu Meng†

Department of Material Science & Engineering, Jinan University, Guangzhou 510632, State Key Laboratory of Coordination Chemistry, Nanjing University, Nanjing 210093, P. R. China

Received October 25, 2006; Revised Manuscript Received December 17, 2006

ABSTRACT: Nanoporous thin films, a promising candidate of spin-on ultralow dielectrics for microelectronic applications, have been fabricated via thermally sacrificing a new pore generator octa(2,4-dinitrophenyl)-silsesquioxane (ODNPSQ) in a higher molecular weight (M_w = 30 872) polyphenylsilsesquioxane (PPSQ) matrix. The organic−inorganic hybrid ODNPSQ exhibits a core−shell structure (one cubic Si_8O_{12} core covered by eight dinitrophenyl groups as shell) with high decomposition temperature at ∼420 °C. PPSQ holds a chain molecular structure consisting of numbered ladderlike and partial T_{12} cagelike repeating units, which could be thermally bonded first via an intermolecular condensation reaction, forming two-dimensional sheets, and then further linked by sharing oxygen atoms, generating a highly cross-linked three-dimensional framework by curing at 450 °C, featuring a single strong FT−IR symmetrical Si−O−Si stretching frequency at 1132 cm^{-1}. Nanopores in PPSQ matrix are imprinted by sacrificing ODNPSQ porogen curing at 450 °C. FT−IR is used to study the interaction and structure changes of PPSQ precursor as a function of curing temperature (ranging from 25 to 500 °C) and porogen loading (ranging from 0 to 40 wt %), and a hydrophilic porogen Tween-20 was also used as a reference to carry out a comparative study with the ODNPSQ porogen. Because of phase separation, the amphiphilic PPSQ precursor has a saturated miscibility with the hydrophilic Tween-20 at 30% porogen loading after curing. However, PPSQ gives a better compatibility with the lipophilic ODNPSQ porogen over 40% porogen loading after curing, and the resulting porous spin-on thin films showed low water absorption (0.45%) and low dielectric constant (1.93).

Introduction

Challenges resulting from decreasing feature sizes in microelectronic devices have led to continuously update requirements for dielectrics materials that have a low dielectric constant and are able to mitigate a substantial increase in interconnect delays (RC delay) caused by the increased line resistance and capacitive coupling and the cross talk between the smaller and more closely spaced wires.[1−5] Recent research shows that the scaling of the feature size of integrated circuits has approached 45 and 32 nm technology nodes and the package density will reach about 10^9 CMOS transistors in 2007.[6] Much effect has been exerted in the development of spin-on low dielectric constant materials that include both synthetic fluorinated[7] and nonfluorinated polymers.[8−12] As fluoropolymers have inadequate thermal stability and potential hydrogen fluoride evolution and reaction with metallurgy for current integration procedures, considerable research interest has been devoted to the nonfluorinated materials (such as polyimides,[8,9] heteroaromatic polymers,[10] hydrocarbon polymers,[11] spin-on aromatic thermosetting polyphenylene,[12] and so on).

Polyalkylsilsesquioxanes,[13] one family of nonfluorinated polymers, are promising candidates for ultralow dielectrics as their inherent low dielectric constant (k = 2.9−2.7), low water uptake (<1%), high thermal stability, and excellent processing ability in gap filling, spin-on filmmaking, planarization, chemical mechanical polishing, and damascene processing.[14] One of effective methods for fabricating ultralow dielectrics is to incorporate voids (k = 1.01) into polyalkylsilsesquioxane matrixes via sacrificing organic supramolecular templates (porogens), which could be ionic surfactants or unimolecular compounds[15−21] such as the linear poly(D,L-lactide)-1,6-hexanediol,[15] poly(styrene-block-2-vinypyridine)[16] and P(MMA-*co*-DMAEMA),[17] the star-shaped poly(ϵ-caprolactone) (PLC),[18] (PCL-4),[19] and (PCL-6),[20] the hyperbranched poly(ϵ-caprolactone),[21] the hyperbranched ketalized polyglycidol (K-PG),[22] and so on. Because of a variety of molecular structures, these porogens exhibit different miscibility with precursors, and their phase behavior in solution or both before and after curing is still not well documented. The amphiphilic polyalkylsilsesquioxanes have good miscibility with hydrophilic porogens in solution before curing but not often after curing. As the condensation reaction of silanol groups in the polyalkylsilsesquioxane during the curing process can change the matrix's nature from amphiphilic to lipophilic, the miscibility between the matrix and hydrophilic porogens will decrease and often result in a phase separation, which is critical for control over the final pore structures and film properties.[23] On the one hand, strong intermolecular interactions (especially hydrogen bonds) between the matrix and porogen often are used as a tool to enhance the miscibility between precursor and porogen. On the other hand, hydrogen bonds in the matrix can also increase the chance of water uptake.[17] As high water uptake can damage dielectric properties of materials and cause corrosion of metallurgy, a further decreasing in water uptake for future ultralow dielectric constant materials is necessary. However, most reported porogens have hydrophilic silanol groups in their molecular out layers[15−22] and they can form strong hydrogen bonds with hydroxyl groups from polyalkylsilsesquioxanes, which benefits the miscibility between precursors and porogens

* Corresponding author. E-mail: thjchen@jnu.edu.cn. Telephone: 86-020-85221362. Fax: 86-020-85223271.

† Department of Material Science & Engineering, Jinan University, Guangzhou 510632, P. R. China.

‡ State Key Laboratory of Coordination Chemistry, Nanjing University, Nanjing 210093, P. R. China..

10.1021/ma062471x CCC: $37.00
Published on Web 02/20/2007

but does not profit the decreasing of moisture absorption in the resulting matrix.[24,25]

With an attempt to reduce moisture absorption in the matrixes, we design a less hydrophilic system, a high-molecular-weight polyphenylsilsesquioxane (PPSQ) as a precursor and a lipophilic octa(2,4-dinitrophenyl)silsesquioxane (ODNPSQ) as a porogen.[26] The organic−inorganic hybrid ODNPSQ has a core−shell structure consisting of one cubic Si_8O_{12} core and eight 2,4-dinitrophenyl groups bonded to the eight silicon atoms as a shell. Because the 2,4-dinitrophenyl group exhibits lipophilic and the core−shell structure's organic−inorganic hybrid has a high decomposition temperature (∼420 °C), it is suitable as a new pore generator for imprinting nanopores in polyalkylsilsesquioxane films. In this work, we use ODNPSQ as porogen to imprint nanopores in PPSQ thin films, investigating miscibility between the precursor and porogen, assessing structural changes of resulting matrix with curing, studying thermal stability, surface topography, moisture absorption, optical, and dielectric properties of the porous thin films. A four-leg-shaped surfactant, polyoxyethylene sorbitan monolaurate (Tween-20), is used as hydrophilic porogen to compare with the lipophilic ODNPSQ in the study.

Results and Discussion

Synthesis and Structure of the Precursor. Sprung and Guenther[27] reported the first synthesis of PPSQ by refluxing phenyltriethoxysilane (PTES) in methyl isobutyl ketone solution containing tetraethylammonium hydroxide and water, and Prodo et al.[28] synthesized PPSQ through hydrolyzing PTES under a pH = 8 aqueous medium and catalyzed by ammonium salts (TPABr or CTABr). Recently, a revised method also was documented by Lee et al.[29] However, it is difficult by these methods to synthesize PPSQ with a molecular weight higher than 10 000.[30] In this work, we prepared a new PPSQ by two-step reactions: first, alcoholyze phenyltrichlorosilane (PTCS) with absolute ethanol to produce stoichiometrically PTES, and then condense PTES further in basic toluene solution through the catalyst of water to produce both 80% of T_8 and ∼20% of PPSQ. GPC analysis of the byproduct PPSQ shows multiple peaks with higher weight-average molecular weight (M_w = 30 872, M_n = 8116) and a wide polydispersity (PDI = 6.7). In the family of polyphenylsilsesquioxanes, a few possible structural types have been reported, such as the cages (T_8, T_{10}, and T_{12}), the partial cagelike chains, and the ladderlike chain.[13,31,32] Because the cages T_8−T_{12} have relatively low molecular weight (1033−1550) and only either the partial cagelike chains or the ladderlike chain or both of them are possible to hold a molecular weight over 10 000. In the FTIR spectra of polyalkylsilsesquioxanes, the Si−OH stretching frequency is located usually at ∼930 cm^{-1}, and its absorbance intensity is proportional to the content of silanol groups in the corresponding polymers.[17] In the FTIR spectra of the titled precursor, only a weak absorbance at 920 cm^{-1} is found, which means that the ratio of silanol group in the polymer is fairly low.[33] However, a very strong absorbance at 1137 cm^{-1} is also found, which agrees with the Si−O−Si characteristic absorption of the T_{12} cage structure.[32] X-ray diffraction of the titled precursor shows one strong peak (2θ = 7.22) and a wide peak (2θ = 18.62), both of them agree with the interpretation of characteristic parameters for crystalline ladderlike polyphenylsilsesquioxane with the mean intermolecular chain−chain distance (intense peak at 2θ = 7.3, $d \approx$ 1.20 nm) and the mean repeat distance of chains (intense peak at 2θ = 19.2, $d \approx$ 0.46 nm),[28,31,33,34] which indicates that the ladderlike chain structure must exist in the titled precursor. Thermal analysis for the titled precursor exhibits the following

Scheme 1

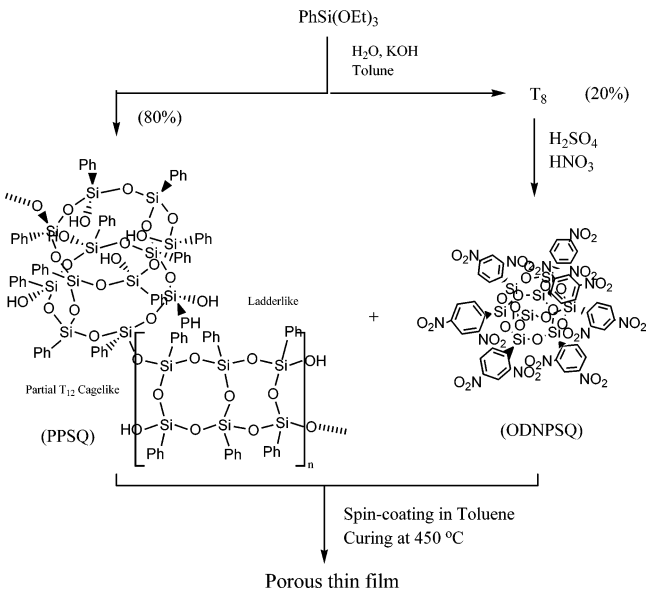

weight loss behavior described in Figure 2. The weight loss begins at ∼480 °C, and the loss drops quickly after the temperature and gives out a residual weight of about 51% until 700 °C, which is higher than the theoretical calculation from the molecular composition $[(C_6H_5)SiO_{1.5}]_n$. Considering that part of silicon atoms in the polymer are bonded to the terminal hydroxyl groups, the residual weight 51% agrees with the theoretical calculation of molecular formula $[(C_6H_5)_{0.9}(OH)_{0.1}SiO_{1.5}]_n$, which suggests that the ratio of hydroxyl groups to phenyl groups in the mixed ladderlike and partial cagelike chain of the precursor is about 1:9. According to the above measurements and analyses, we conclude that the molecular structure of the titled precursor is a mixed ladderlike and partial cagelike chain, as described in Scheme 1.

Structural Transfers of PPSQ Thin Films at Curing. The linear precursor is soluble in organic solvents toluene, xylene, methyl isobutyl ketone, tetrahydrofuran, and acetone, but it can form fine thin films only in the former three solvents. All curing processes for the precursor were carried out under nitrogen gas in a changing temperature range of 60−500 °C. Structural changes involve both chain extension and chain cross-linking, by which the precursor is ultimately linked together to form a high cross-linking covalent framework. Both chain extension and chain cross-linking occur through the following two main condensation reactions: (1) two terminal HO−Si− groups lose one water molecule to form one −Si−O−Si− unit; (2) one terminal HO−Si− group and one terminal phenyl−Si− group lose one benzene molecule, forming one −Si−O−Si− unit. In the FT−IR spectra of the precursor, the disappearance of stretching absorptions at 920 cm^{-1} happened at 150 °C, which indicates the first condensation reaction.[17] The stretching absorptions in 1000−1200 cm^{-1}, usually a strong doublet peak with the high frequency in the 1115−1150 cm^{-1} region and a low frequency in the 1000−1080 cm^{-1} region, are the characteristic stretching frequencies of Si−O−Si units, and they are able to give out significant structural information in polyalkylsilsesquioxane matrixes.[34−37] The Si−O−Si stretching absorptions of the titled precursor at room temperature were found at both 1132 and 1047 cm^{-1}, and their relative intensities changed with the curing temperature increasing (Figure 1). According to Bornhauser' research for PMSQ curing at different temperatures,[35] the cagelike structure should show a stronger Si−O−Si stretching absorption in a high-frequency region and the

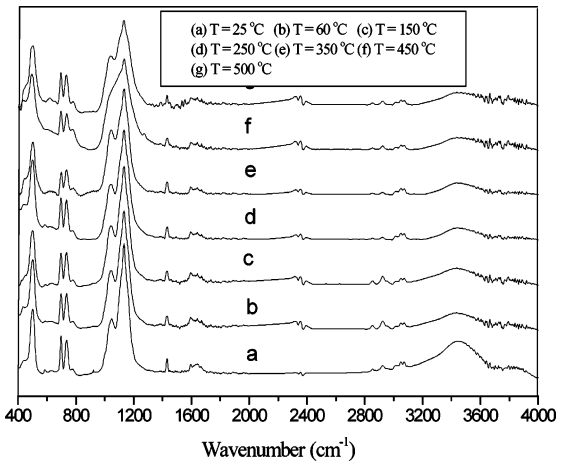

Figure 1. FTIR spectra of PPSQ precursor as a function of curing temperature.

ladderlike structure should show a weaker Si−O−Si stretching absorption in a low-frequency region. Following the point of view, Huang et al. enhanced the concept by proposing an absorption ratio of the low frequency to high frequency to measure the cross-linking of Si−O−Si bands as a function of curing temperature.[32] Another explanation from Wang et al.[38] suggested that the terminal silicon group consisting of nonbridging oxygen atoms (O_{nb}) also could exhibit high-frequency Si−O−Si bands. The FT−IR spectra of the titled PPSQ as a function of curing temperature show a distinct change from the low frequency to high frequency of Si−O−Si bands. The disappearance of the low-frequency Si−O−Si band (1047 cm^{-1}) at 450 °C means the loss of the ladderlike structures, and the enhancing of the high-frequency band (1132 cm^{-1}) express a structural transfer toward partial cagelike structures. With the rising of curing temperature, the second condensation reaction happens and the cross-linking of chains increases, the mixture chains are transferred first into 2-D sheets and then a 3-D framework, giving a single high-frequency band at 1132 cm^{-1}, which is consistent with the characteristic absorption of T_{12} cage structure.[33]

Thermal Decomposition Behavior of the Porogens at Curing. Because the initial decomposition temperature of ODNPSQ porogen (420 °C) is so close to the curing temperature (450 °C), we used a commercial nonionic surfactant Tween-20 as porogen to investigate the thermal decomposition behavior in the matrix. The porogen Tween-20 has a initial decomposition temperature at ∼200 °C, which is higher than the starting cross-linking temperature of the precursor at 150 °C (Figure 2). This is favorable for the multistep curing process and is able to prevent the pores formed in the matrix from collapsing due to the capillary pressures from the decomposition of the porogen.[15,19,20,22] The thermal decomposition of the precursor with Tween-20 porogen loading occurred in two distinct steps: the first step begins at the temperature range of 200−350 °C with a loss weight 30−40%, which are associated with the loss of the porogen with the corresponding loading levels; the second step shows a complete sacrifice of the porogen in the matrix at 450 °C. Similarly, with Tween-20, when the curing process was carried out at 450 °C, the ODNPSQ porogen decomposed completely. At this temperature, the mixed ladderlike and partial cagelike chains were allowed to slowly self-organize and further cross-linked into a more symmetric geometry framework featuring the partial T_{12} cagelike structure, which can be further proved by the FT−IR spectrum of PPSQ with 10% ODNPSQ porogen loading curing at 450 °C (Figure 3).

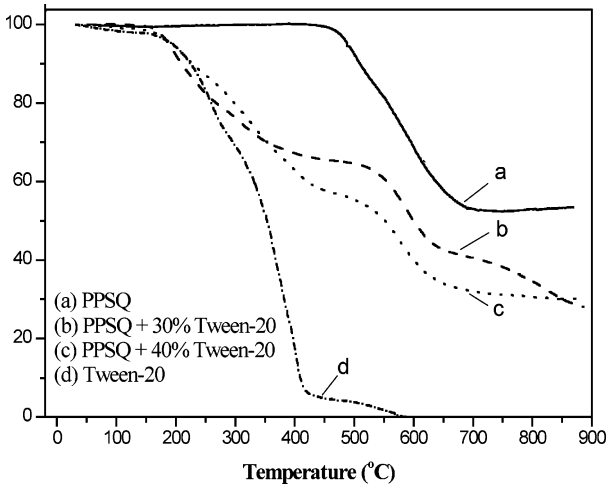

Figure 2. TGA analysis of the PPSQ, Tween-20, and the PPSQ with Tween-20 loading, respectively.

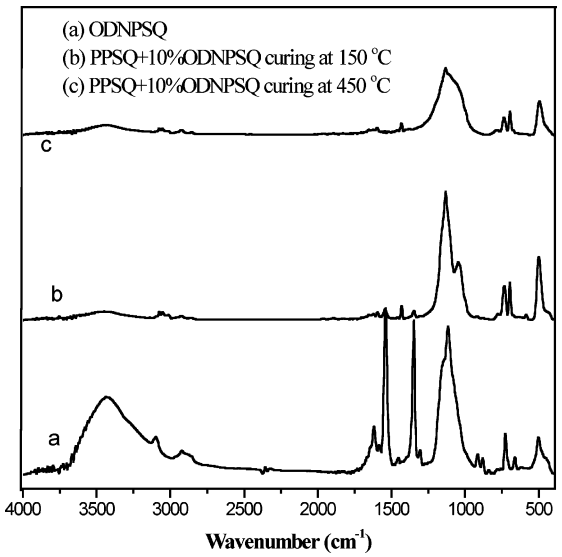

Figure 3. FTIR spectra of ODNPSQ porogen (curve a) and PPSQ with 10% ODNPSQ loading curing at 150 and 450 °C (curve b and c).

Water Absorption. As water uptake in a matrix often leads to the increasing of dielectric constant and corrosion of metallurgy,[14,17] low water absorption is a critical requirement for low dielectric constant materials.[3] The water uptakes of all PPSQ thin film samples curing at different temperatures were measured by using quartz crystal microbalance (QCM) techniques, and the results are shown in Figure 4. The initial value of water uptake of the PPSQ thin film curing at 150 °C is 0.32%. The value decreases gradually to 0.22% with the curing temperature rising to 450 °C and then increases quickly to 1.12 from 450 to 550 °C. The changing tendency of the water uptake of the PPSQ thin film is reverse proportional to that of dielectric constants in the temperature range 150−450 °C. Two features are apparent: first, the PPSQ thin films give relatively lower water absorption than that of PMSQ, which means that an increase in molecular weight and the introduction of a lipophilic phenyl group are favorable for lowing water absorption; second, the PPSQ thin film curing at 450 °C exhibits a minimum of water uptake. We attribute the properties of smallest water uptake and highest dielectric constant for the PPSQ thin film curing at 450 °C to its structural feature.

The water absorption behavior of porous thin films fabricated by PPSQ precursor and Tween-20/ODNPSQ porogens is shown in Figure 5. It was found that the water uptake of porous thin

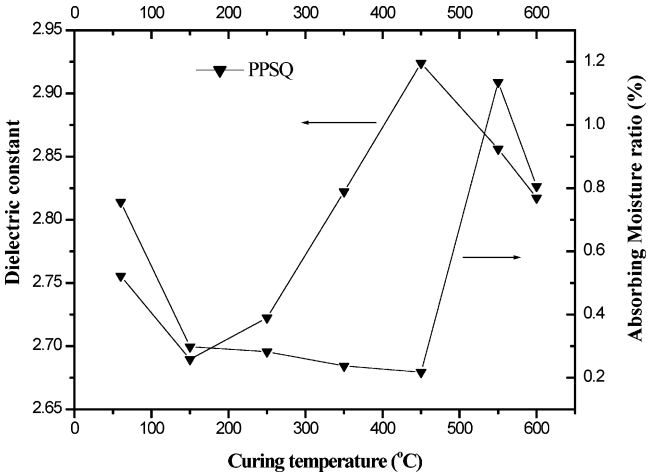

Figure 4. Plot of dielectric constant and absorbing moisture ratio of PPSQ thin films with the curing temperature changing.

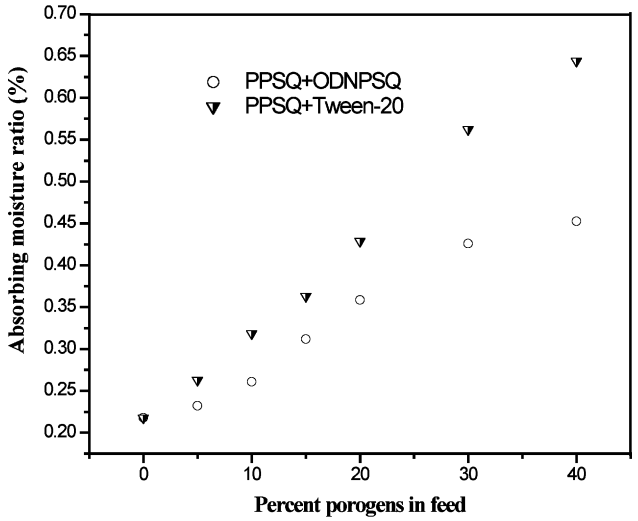

Figure 5. Plot of absorbing moisture ratio of porous PPSQ thin films with the porogens loading curing at 450 °C for 2 h.

films with Tween-20 porogen loading increasing from 0 to 40% increases linearly from 0.22 to 0.63%. However, the water uptake of porous thin films from the ODNPSQ porogen loading increases relatively more slowly than that of Tween-20, giving 0.45% water uptake at 40% ODNPSQ porogen loading. The lipophilic ODNPSQ porogen can decrease formation of possible hydrogen bonds and improve water absorption behavior in a porous PPSQ matrix.

Surface Morphology. The SEM image of PPSQ thin film in Figure 6 shows a very uniform thin film, and the TEM micrograph of porous thin film of PPSQ with 20% ODNPSQ loading curing at 450 °C in Figure 7 shows structural changes in the matrix.

All samples of porous thin films were analyzed by a tapping mode of atomic force microscopy. Parts a−d of Figure 8 show the AFM micrographs of the prepared porous thin films of PPSQ with Tween-20 porogen 10−40% loading, respectively. The porous films in Figure 8a−c show uniform spherical pores and their surface roughness increases with the porogen loading ranging from 10 to 30%, showing nanopores (5−10 nm) in Figure 8c. The cause of pore sizes being larger than the single molecular size of the porogen comes from the interaction of hydrogen bonds and self-aggregation among the porogens. When the Tween-20 porogen loads up to a high content (40%), the AFM micrograph (Figure 8d) shows a significant aggregation

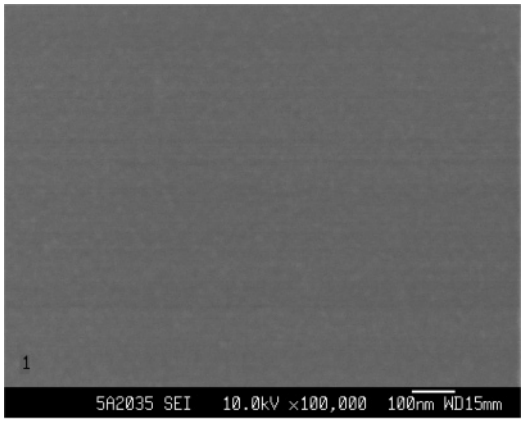

Figure 6. SEM image of PPSQ thin film curing at 450 °C.

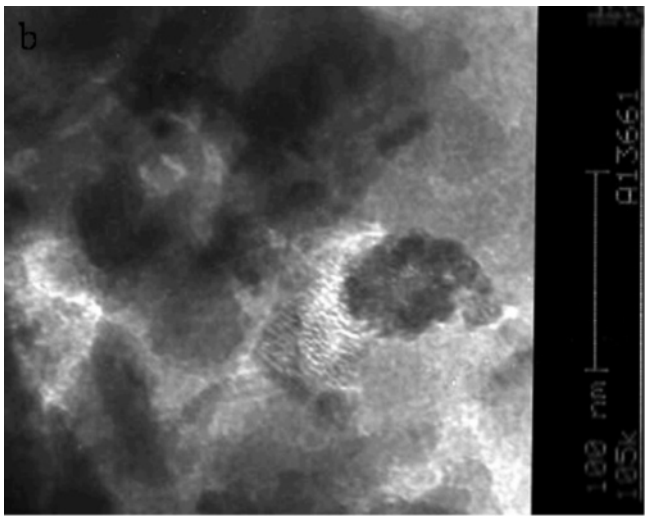

Figure 7. TEM micrograph of porous thin film of PPSQ with 20% ODNPSQ loading curing at 450 °C.

domain and a channel-like structure. Hence, the above results suggest a phase separation in the system resulting from the poor miscibility/compatibility between the amphiphilic precursor and hydrophilic porogen after curing.[18,19,39,40]

Parts a−d of Figure 9 show the AFM diagrams of the prepared porous PPSQ thin films imprinted by ODNPSQ loading ranging from 10 to 40%. Different from the porous PPSQ films from Tween-20 porogen, all porous thin films show continuous phase and all surface roughness of porous PPSQ thin films are higher than that from Tween-20 porogen. The surface roughness of porous PPSQ thin films goes up as the porogen content increases. The AFM micrograph (Figure 8d) gives more regular structure, but neither obvious nanopores nor significant aggregation domain was observed in the AFM diagrams. Because of a small molecular size (~0.65 nm) and lack of hydrophilic groups, the porogen ODNPSQ is not able to self-aggregate through hydrogen bonds growing up into domains. The pores sizes are too small (d < 1.00 nm) to be observed in the measurement. The above results show a good miscibility/compatibility between the amphiphilic precursor and lipophilic porogen in solution and both before and after curing.

Optical and Dielectric Constants. The refractive index properties of all thin films were investigated on a spectroscopic ellipsometry by using the previous reported method at 632.6 nm wavelengths, and corresponding dielectric constants (k) of them were estimated according to the well-known Maxwell−Garnett equation.[17,22] The curve of the dielectric constant of PPSQ thin film vs curing temperature is given in Figure 4. The

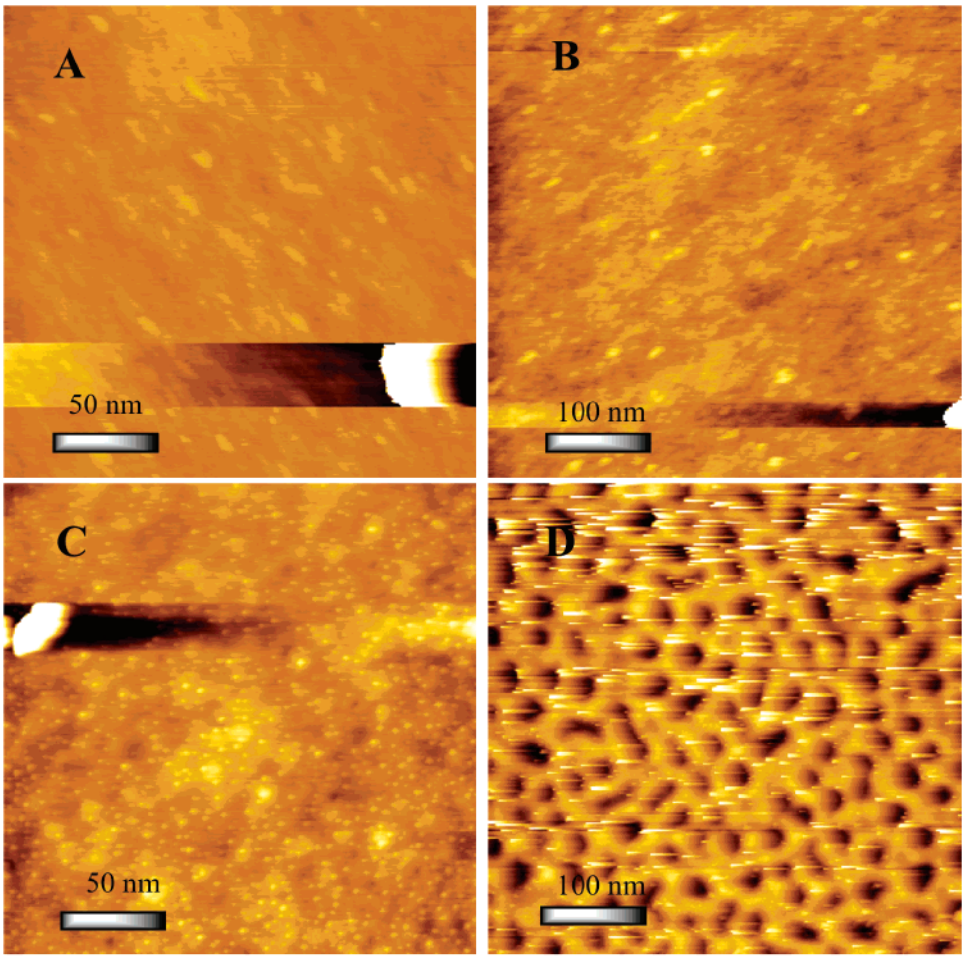

Figure 8. AFM micrographs of mixture of PPSQ and porogen with Tween-20 loading curing at 450 °C for 2 h: (a) 10% Tween-20 loading in PPSQ; (b) 20% Tween-20 loading in PPSQ; (c) 30% Tween-20 loading in PPSQ; (d) 40% Tween-20 loading in PPSQ.

thin film has an initial dielectric constant 2.75 at baking temperature 60 °C and the lowest dielectric constant 2.70 at the curing temperature 150 °C. With curing temperature rising from 150 to 450 °C, the value of the dielectric constant increases and arrives at a maximum 2.9 at curing temperature 450 °C and then decrease back to 2.85 at 500 °C.

The refractive indexes and corresponding dielectric constants of the porous PPSQ thin films versus porogen loading content are given in Figure 10 and Figure 11. The dielectric constants of porous PPSQ thin films with Tween-20 porogen loading ranging from 5 to 30% decrease slowly from 2.63 to 2.02, showing a reversible proportional relationship between dielectric constant and porogen loading. However, the corresponding dielectric constant increases to 2.10 when the Tween-20 loading amount increase up to 40%. On the other hand, the dielectric constants of the porous PPSQ thin films with the ODNPSQ porogen loading from 5 to 40% showed a linear decreasing from 2.66 to 1.93 at 632.6 nm wavelengths, showing a linear relationship between the dielectric constants and the loading amount of ODNPSQ up to 40%.

The porosities of the porous PPSQ thin films generated by pore generators Tween-20 and or ODNPSQ were investigated and estimated by the Lorentz−Lorenz relationship.[36,37] Herein, n and n_o are the refractive indexes of the matrix skeleton and the porous thin film, respectively, and P is the porosity.

$$\frac{n_0^2 - 1}{n_0^2 + 2}(1 - P) = \frac{n^2 - 1}{n^2 + 2} \qquad (1)$$

The results are shown in Figure 11. First, the porosities of the porous PPSQ thin films with the Tween-20 porogen loading from 5 to 30% increase linearly to a maximum 31.5% and then decrease back to 27.2% when the loading amount of the porogen increases up to 40%. However, the porosities of the porous PPSQ thin films with the ODNPSQ porogen loading from 5 to 40% show an apparent linear increase from 3.6 to 35.8%. The sacrificial thermal decomposition of the ODNPSQ porogen successfully imprints pores in the PPSQ matrix.

Conclusion

A condensation reaction of PTES catalyzed by water in a basic toluene solution can produce high-molecular-weight PPSQ at ∼20% yield. The molecular structure of PPSQ exhibits a mixed ladderlike and partial T_{12} cagelike chain, which can be cross-linked into a three-dimensional covalent framework containing partial T_{12} cagelike repeating units and characterized by a strong FT−IR symmetrical Si−O−Si stretching frequency at 1132 cm^{-1}. Comparing the properties of PPSQ thin film materials curing at a range from 25 to 500 °C, the material constructed from the titled PPSQ curing at 450 °C shows the highest dielectric constant and lowest water uptake, which means that the best curing temperature to generate a partial T_{12} cagelike three-dimensional framework is 450 °C. The phase separation happening in the system of PPSQ and 40% Tween-20 loading results from the poor miscibility/compatibility between the amphiphilic PPSQ precursor and the hydrophilic Tween-20 porogen. The organic−inorganic hybrid ODNPSQ, with a core−shell-shaped structure and a decomposition temperature (420

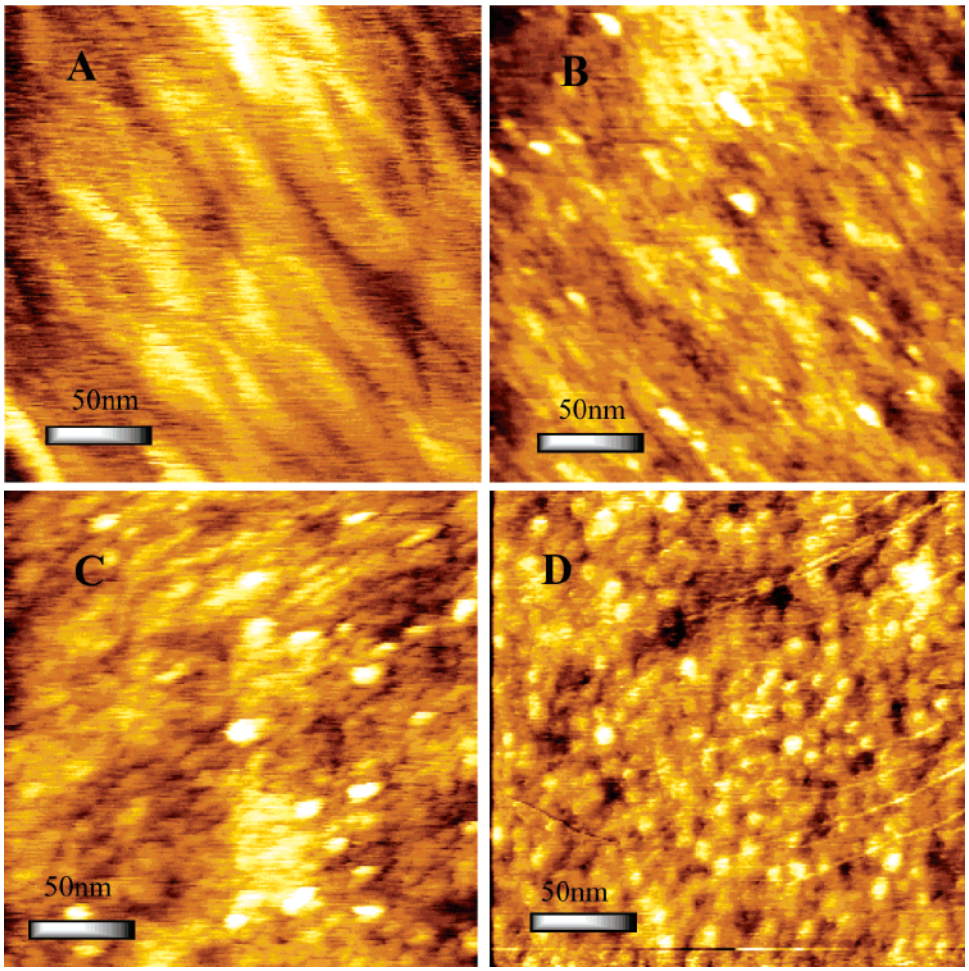

Figure 9. AFM micrographs of mixture of PPSQ and porogen with ODNPSQ loading curing at 450 °C for 2 h: (a) 5% ODNPSQ loading in PPSQ; (b) 20% ODNPSQ loading in PPSQ; (c) 30% ODNPSQ loading in PPSQ; (d) 40% ODNPSQ loading in PPSQ.

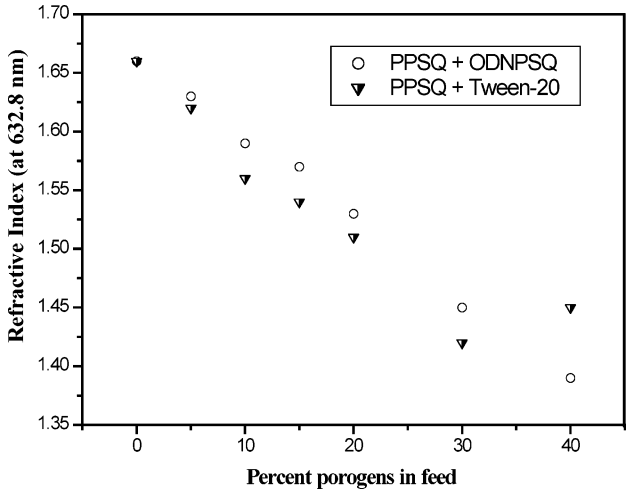

Figure 10. Refractive index of porous PPSQ thin films vs porogens loading.

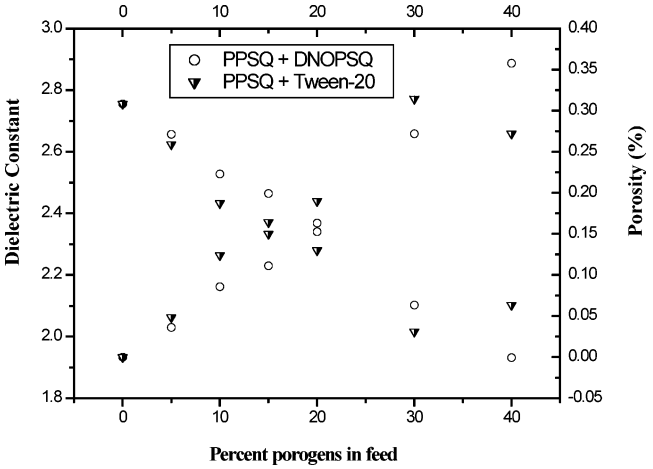

Figure 11. Plot of dielectric constant and porosity of porous thin films vs the different porogens (Tween-20 and ODNPSQ) loading in PPSQ.

°C), is able to be used as a lipophilic porogen to imprint nanosized pores in the PPSQ matrix, and the resulting porous materials exhibit a low water absorption (0.45%) and dielectric constant (1.93). The above results offer an effective approach for us to improve both miscibility/compatibility and water absorption behavior for the low dielectric constant materials from polyalkylsilsesquioxanes. The increase of molecular weight for the polyphenylsilsesquioxane precursor and the introduction of the lipophilic ODNPSQ porogen generated a less hydrophilic system and decreased the forming of hydrogen bonds. These porous PPSQ thin films are one of promising candidates of ultralow dielectrics for fabricating integrated circuit chips in advanced microelectronic devices.

Acknowledgment. This work was supported by the Natural Science Startup Foundation of Jinan University, (no. 51204005) and the Natural Science Foundation of Guangdong Province (no. 0430064), People's Republic of China. We also thank the initial research supporting from Professor Rechard M. Laine,

Department of Material Science and Engineering, University of Michigan.

Supporting Information Available: Experimental section. This material is available free of charge via the Internet at http://pubs.acs.org.

References and Notes

(1) *The International Technology Roadmap for Semiconductors*; International SEMATECH: Austin, TX, 2002.
(2) *The National Technology Roadmap for Semiconductors*; Semiconductor Industry Association: San Jose, CA, 1997.
(3) Miller, R. D. *Science* **1999**, *286*, 421.
(4) Leo, C. M.; Chang, Y. T.; Wei, K. H. *Chem. Mater.* **2003**, *15*, 3721.
(5) Baskaran, S.; Liu, J.; Domansky, K.; Kohler, N.; Li, X.; Coyle, C.; Fryxell, G. E.; Thevuthasan, S.; Williford, R. E. *Adv. Mater.* **2000**, *12*, 291.
(6) Vu Ho, V.; Scansen, D.; Keyes, E. *Semicond. Int.* **2003**, *26*, 56.
(7) Carter, K. R.; DiPietro, R. A.; Sanchez, M. I.; Swanson, S. A. *Chem. Mater*. **2001**, *13*, 213.
(8) Watanabe, Y.; Shibasaki, Y.; Ando, S.; Ueda, M. *Polymer* **2005**, *46*, 5903.
(9) Hedrick, J. L.; Miller, R. D.; Hawker, C. J.; Carter, K. R.; Volkson, W.; Yoon, D. Y.; Trollsas, M. *Adv. Mater.* **1998**, *10*, 1049.
(10) Huang, Y.; Economy, J. *Macromolecules* **2006**, *39*, 1850.
(11) Kosuge, K.; Kikukawa, N.; Takemori, M. *Chem. Mater*. **2004**, *16*, 4181.
(12) Martin, S. J.; Godschals, J. P.; Mills, M. E.; Shaffer, E. O., II; Townsend, P. H. *Adv. Mater.* **2000**, *12*, 1769.
(13) Baney, R. H.; Itoh, M.; Sakakibara, A.; Suzuki, T. *Chem. Rev*. **1995**, *95*, 1409.
(14) K. Maexa, K.; Baklanov, M. R.; D. Shamiryan, D.; Iacopi, F.; Brongersma, S. H.; Yanovitskaya, Z. S. *J. Appl. Phys.* **2003**, *93*, 8793.
(15) Hong, S. M.; Hwang, S. S. *J. Appl. Polym. Sci.* **2006**, *100*, 4964.
(16) Yang, C. C.; Wu, P. T.; Chen, W. C.; Chen, H. L. *Polymer* **2004**, *45*, 5691.
(17) Huang, Q. R.; Vilksen, W.; Huang, E.; Toney, M.; Frank, C. W.; Miller, R. D. *Chem. Mater* **2002**, *14*, 3676.
(18) Nguyen, C. N.; Carter, K. R.; Hawker, C. J.; Hedrick, J. L.; Jaffe, R. L.; Miller, R. D.; Remenar, J. F.; Rhee, H.-W.; Rice, P. M.; Toney, M. F.; Trollsås, M.; Yoon, D. Y. *Chem. Mater.* **1999**, *11*, 3080.
(19) Oh, W.; Hwang, Y.; Park, Y. H.; Ree, M.; Chu, S.-H.; Char, K.; Lee, J. K.; Kim, S. Y. *Polymer* **2003**, *44*, 2519.
(20) Lee, B.; Oh, W.; Hwang, Y.; Park. Y.-H.; Yoon, J.; Jin, K. S.; Heo, K.; Kim, J.; Kim, K.-W.; Ree, M. *Adv. Mater.* **2005**, *17*, 696.
(21) Nguyen, C. J.; Hawker, R. D.; Miller, E.; Huang, E.; Hedrick, J. L. *Macromolecules* **2000**, *33*, 4281.
(22) Kim, J.-S.; Kim, H.-C.; Lee, B.; Ree, M. *Polymer* **2005**, *46*, 7394.
(23) Alexandridis, P.; Holzwarth, J. F.; Hatton, T. A. *Macromolecules* **1994**, *27*, 2414.
(24) Ying, J. Y.; Mehnert, C. P.; Wong, M. S. *Angew. Chem., Int. Ed.* **1999**, *38*, 56.
(25) Li, G. Z.; Wang, L.; Toghiani, H.; Daulton, T. L.; Koyama, K.; Pittman, C. U., Jr. *Macromolecules* **2001**, *34*, 8686.
(26) Chen, H.-J. *Chem. Res. Chin. Univ.* **2004**, *20*, 42.
(27) Sprung, M. M.; Guenther, F. O. *J. Polym. Sci.* **1958**, *28*, 17.
(28) Prado, L. A. S. A.; Radovanovic, E.; Pastore, H. O.; Yoshida, I. V. P. Torriani, I. L. *J. Polym. Sci., Part A: Polym. Chem.* **2000**, *38*, 1580.
(29) Lee, E. C.; Kimura, Y. *Polym. J.* **1998**, *30*, 730.
(30) Yamamoto, S.; Yasuda, N.; Ueyama, A.; Adachi, H.; Ishikawa, M. *Macromolecules* **2004**, *37*, 2775.
(31) Brown, J. F., Jr.; Vogt, J. H., Jr.; Katchman, A.; Eutance, J. W.; Kiser, K. M.; Krantz, K. W. *J. Am. Chem. Soc*. **1960**, *82*, 6194.
(32) Brown, J. F., Jr.; Vogt, J. H., Jr.; Prescott, P. I. *J. Am. Chem. Soc.* **1964**, *86*, 1120.
(33) Kumaraswamy, G.; Deshmukh, Y.; Agrawal, V. V.; Rajmohanan, P. *J. Phys. Chem. B* **2005**, *109*, 16034.
(34) Liu, C.; Liu, Y.; Shen, Z.; Xie, P.; Zhang, R.; Yang, J.; Bai, F. *Macromol. Chem. Phys.* **2001**, *202*, 1581.
(35) Wang, C. Y.; Shen, Z. X.; Zheng, J. Z. *Appl. Spectrosc.* **2000**, *54*, 209.
(36) Lorentz, H. A. *Wied. Ann. Phys. Chem.* **1880**, *9*, 641.
(37) Lorentz, L. V. *Wied. Ann. Phys. Chem.* **1880**, *11*, 70.
(38) Wang, C. Y.; Shen, Z. X.; Zheng, J. Z. *Appl. Spectrosc.* **2001**, *55*, 1347.
(39) Huang, Q. R.; Frank, C. W.; Mecerreyes, D.; Vilksen, W.; Miller, R. D. *Chem. Mater.* **2005**, *17*, 1521.
(40) Yang, S.; Mirau, P. A.; Pai, C.-S.; Nalamasu, O.; Reichmanis, E.; Lin, E. K.; Lee, H.-J.; Gidley, D. W.; Sun, J. *Chem. Mater.* **2001**, *13*, 2762.

MA062471X